Eur. Phys. J. C 32, 385–397 (2004)
Digital Object Identifier (DOI) 10.1140/epjc/s2003-01416-9

THE EUROPEAN PHYSICAL JOURNAL C

The baryonic Y-shape confining potential energy and its approximants

B. Silvestre-Brac[1,a], C. Semay[2,b], I.M. Narodetskii[3,c], A.I. Veselov[3,d]

[1] Laboratoire de Physique Subatomique et de Cosmologie, Av. des Martyrs 53, 38026 Grenoble-Cedex, France
[2] Université de Mons-Hainaut, Place du Parc 20, 7000 Mons, Belgium
[3] Institute of Theoretical and Experimental Physics, B. Cheremushkinskaya 25, 117218 Moscow, Russia

Received: 23 June 2003 / Revised version: 15 September 2003 /
Published online: 3 December 2003 –

Abstract. We discuss the validity of replacing the complicated three-body confinement operator of the Y string junction type by three kinds of approximation which are numerically much simpler to handle: a one-body operator with the junction point at the centre of mass, a two-body operator corresponding to half the perimeter of the triangle formed by the three particles, and the average of both. Two different approaches for testing the quality of the approximations are proposed: a geometrical treatment based on the comparison of the potential energy strengths for the various inter-quark distances, and a dynamical treatment based on the comparison of the corresponding effective string tensions using a hyperspherical approach. Both procedures give very similar results. It is shown how to simulate the genuine string junction operator by the approximations proposed above. Exact three-body calculations are presented in order to compare quantitatively the various approximations and to confirm our analysis.

1 The Y string potential and possible approximations

The QCD lattice calculations support the idea that the confining potential energy in a three quark system can be, at best, simulated by the so-called Y-shape potential [1]. In this scheme, the three point-like quarks (located at the apices of a triangle ABC), are connected by three flux tubes starting from a junction point (I) in such a manner that it minimises the sum of the distances to the three quark positions. Note that effective QCD theories support also this idea [2].

If the angle corresponding to an apex is greater than 120°, the junction point is precisely at this apex, whereas if all the angles are less than 120°, then the equilibrium junction position coincides with the so-called Toricelli (or Fermat or Steiner) point; it corresponds to a point for which the corresponding angles $\widehat{AIB}$, $\widehat{BIC}$, and $\widehat{AIC}$ are all equal to 120°.

Thus the genuine string potential in a baryon is defined by

$$V_Y = \sigma(AB + AC) \quad \text{if} \quad \widehat{A} > 120^\circ$$
$$(+ \text{ circular permutation on } B \text{ and } C),$$
$$V_Y = \sigma(IA + IB + IC) \quad \text{if} \quad \widehat{A}, \widehat{B}, \widehat{C} \leq 120^\circ, \tag{1}$$

where σ is the string tension, in principle a constant of the theory. This expression has been used in several works (see for instance [3–6]). The success of simple quark models using a potential to simulate the confinement without gluonic modes can be justified by the fact that the lowest gluonic excitation energy in the three quark system is found to be about 1 GeV in the hadronic scale [10].

Efficient methods to deal with Y-shape interaction rely either on Monte-Carlo algorithms (see for instance [7, 8]) or hyperspherical methods (see for instance [9]). However it is very difficult to implement in a numerical code, essentially for two reasons:
(i) it is a three-body operator which makes the equations very complicated;
(ii) the presence of two different expressions depending upon the configuration makes the integration domain not evident to handle. This complexity explains why, for practical calculations, the genuine Y-shape potential is often replaced by other expressions that are considered as approximants.

The most popular one is to consider half the perimeter of the triangle formed by the three quark coordinates and to define the confining potential as

$$V_C = \frac{\sigma}{2}(AB + BC + CA), \tag{2}$$

which is also called the Δ-shape potential. However it is shown in [1] that the three quark potential energy is better

[a] e-mail: silvestre@lpsc.in2p3.fr
[b] FNRS Research Associate;
e-mail: claude.semay@umh.ac.be
[c] e-mail: naro@heron.itep.ru
[d] e-mail: veselov@heron.itep.ru

represented by the Y-shape interaction than by the Δ-shape one. Nevertheless, the potential (2) is a two-body operator, free from the complication due to angles; hence it is much simpler and it is still widely used in practice (see for instance [11–13]).

A $\boldsymbol{\lambda}_i \cdot \boldsymbol{\lambda}_j$ colour dependence associated with a two-body linear confinement does produce such a 1/2 factor. Although this colour prescription is perfectly relevant in the case of one-gluon exchange, there is no theoretical justification to apply it for the confinement potential. This 1/2 factor is close to the value 0.53, predicted by lattice calculation [1], if one tries to replace the Y-shape by a Δ-shape.

It is very important to stress that both the genuine string potential (1) and the two-body confining potential (2) are of geometrical essence, depending only on the position of the quarks and being independent of their masses.

Another approximation that was suggested is to replace the true junction point I by the centre of mass G of the three quark system [14,15]. In this case the corresponding confining operator is simply

$$V_G = \sigma(GA + GB + GC). \tag{3}$$

This approximation is particularly interesting since this potential is a one-body operator free from angle complications; hence its numerical treatment is quite easy. In contrast to the previous expressions, this approximation does depend on the system via the centre of mass coordinate.

In this paper, assuming that V_Y represents the true physics, we want to study the quality of the approximations (2) and (3) and their relevance. To this end, we propose two approaches: a geometrical one and a dynamical one relying on the hypercentral formalism. With this latter technique, it is possible to obtain directly an average value of the confining potential energy depending only on one length parameter. Then we check their validity with an exact three-body treatment based on a complete hyperspherical treatment (beyond the hypercentral approximation). A simulation of three-body potential by sums of two-body potentials was performed in [16], but with a philosophy very different from the one developed here.

In the next section, the geometrical approach is presented. In Sect. 3, the hyperspherical formalism is used to calculate the value of the effective string tension for a given system. Section 4 is devoted to a three-body treatment of the confining potential and the simulation of the genuine string operator. Conclusions are drawn in the last section.

2 Geometrical approach

2.1 Configuration of the system

We are interested in the ratio of the potential energy for two forms of confining interactions as function of the configuration of the system. Since this ratio is scale independent and since the dynamical constant σ disappears in this ratio, it is always possible to rescale the quark triangle putting $AB = 1$ and to deal only with the remaining apex of the triangle. Denoting by L the minimal distance from the junction point I, by D the distance from the centre of mass G, and by P half the perimeter of the triangle, we will study the ratios $R_{Y/C} = V_Y/V_C = L/P$, $R_{G/C} = V_G/V_C = D/P$, $R_{G/Y} = V_G/V_Y = D/L$.

In order to obtain analytical expressions (already complicated!) for these ratios we restrict ourselves to a system with 2 identical quarks of mass m located in A and B and a third one of mass $M = xm$ located in C. The region $0 < x < 1$ corresponds to QQq systems with a light and two heavy quarks; the region $x > 1$ corresponds to qqQ systems with a heavy and two light quarks. The case $x = 1$ corresponds to systems qqq with three identical masses.

Since AB is fixed, the only freedom for the geometry of the system is the position of the apex C, that can be defined by two angles $a = \widehat{A}$ and $b = \widehat{B}$. Following the previous remarks, one must calculate $L(a,b), P(a,b), D(a,b,x)$. In fact this study is still too complicated. One can simplify it a lot noting that there is a symmetry versus the mediating line of AB, with the consequence that $R(a,b) = R(b,a)$. This implies that an extremum of those ratios, the only important thing for our consideration, always lies in the mediating line and it is sufficient to restrict the study to isosceles triangles. Thus, we only compute $R_{Y/C}(a), R_{G/C}(a,x)$ and $R_{G/Y}(a,x)$.

In a quantum mechanical treatment of the confinement, the wave function of course explores all the configurations for the triangle so that, maybe, the most important physical quantity to be computed is the average of the previous ratios. One defines

$$R(x) = \frac{2}{\pi} \int_0^{\pi/2} R(a,x)\, \mathrm{d}a. \tag{4}$$

2.2 Various distances

The calculation of the various distances results from geometrical properties in a triangle and presents no difficulty. It is easy to show the following.

(1) The genuine string distance is given by

$$L(a) = \frac{1}{\cos(a)} \quad \text{if} \quad 0 \le a \le \pi/6, \tag{5a}$$

$$L(a) = \frac{1}{2}(\tan(a) + \sqrt{3}) \quad \text{if} \quad \pi/6 < a < \pi/2. \tag{5b}$$

(2) Half the perimeter is equal to

$$P(a) = \frac{1 + \cos(a)}{2\cos(a)}. \tag{6}$$

(3) The centre of mass string distance is given by

$$D(a,x) = \frac{\tan(a) + \sqrt{x^2 \tan^2(a) + (2+x)^2}}{2+x}. \tag{7}$$

2.3 Genuine potential to half perimeter

With the expressions (5) and (6), one has $R_{Y/C}(a) = L(a)/P(a)$. This ratio is always larger than 1, meaning that the genuine string junction potential is always more repulsive than the sum of the two-body confining potentials. However, the ratio is 1 for a flat triangle or for an infinitely stretched triangle and presents a maximum, $2/\sqrt{3} \approx 1.155$, for an equilateral triangle. This is in agreement with the result of [1].

The average value (4) in this case is equal to

$$R_{Y/C} = \frac{2}{\sqrt{3}} + \frac{2}{\pi}\left[1 - \sqrt{3} + 2\ln\left(\frac{1+\sqrt{3}}{2}\right)\right] \approx 1.086. \tag{8}$$

The value $1/2\,R_{Y/C} \approx 0.54$ must be compared with the corresponding value 0.53 derived from QCD [1]. Thus the average error replacing the string tension operator by the sum of the two-body confining potentials is of the order of 8%; this approximation can be considered as a good one.

2.4 Centre of mass junction approximation to half perimeter

There does not exist special angle conditions in this case and, following the formulas (7) and (6), the ratio is given by $R_{G/C}(a,x) = D(a,x)/P(a)$.

The maximum value is obtained for an infinitely stretched triangle and for an infinite mass asymmetry. In this special case, the ratio equals 2, but in the physical part of the domain, this ratio is much closer to unity. A more reliable estimation results from averaging following the procedure (4). The integral is cumbersome but can be evaluated analytically using for example the Mathematica package:

$$R_{G/C}(x) = \frac{4}{\pi(2+x)} \times \Big\{\ln(2) + x + 2\sqrt{1+x}\,\arctan\left(2\sqrt{(1+x)}/x\right) - (2+x)\,E(X) + x^2\,K(X)/(2+x)\Big\}, \tag{9a}$$

where

$$X = \frac{4(1+x)}{(2+x)^2}, \tag{9b}$$

and where $K(X)$ and $E(X)$ are the complete elliptic integrals respectively of the first and of the second kinds [17]. The function $R_{G/C}(x)$ is presented in Fig. 1. It is always greater than 1, indicating that the centre of mass string always overestimates the sum of the two-body confining potentials. For $x = 0$ (QQq systems) the value is 1.168, for $x = 1$ (qqq systems) it is 1.136, and for $x = 20$ (qqQ systems) it is 1.248. Curiously it passes through a minimum, 1.132, for $x \approx 0.600$ corresponding to the *ssu* and *ssd* systems. Replacing the two-body potential by the centre of mass string induces an error of about 15–20%.

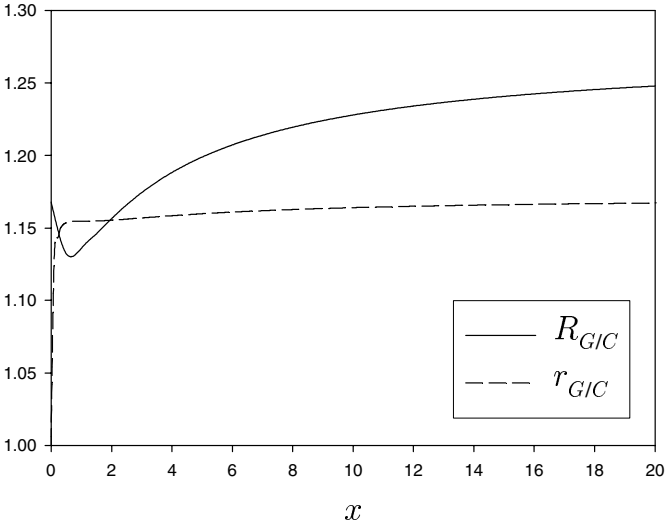

Fig. 1. Ratio $R_{G/C}(x)$ from the geometrical treatment (see formula (9)) and ratio $r_{G/C}(x) = b_G(x)/b_C(x)$ from the hyperspherical treatment (see formulas (34) and (35)), as a function of the mass ratio x

2.5 Centre of mass junction approximation to genuine potential

In a similar way, we define the ratio $R_{G/Y}(a,x) = D(a,x)/L(a)$. A maximum value of 2 is obtained in the very extreme situation $a \to \pi/2$, $x \to \infty$, but, in general, the values of this ratio are very close to 1.

The integration of the expressions $R_{Y/C}(a)$ over the angle a is very cumbersome; the final result looks like

$$R_{G/Y}(x) = \frac{4}{\pi(2+x)} \times \left\{\frac{1}{12}\left(\pi + 3\sqrt{3}\ln(2)\right) + \frac{2-\sqrt{3}}{4} + \frac{2+x}{2}\,E(\pi/6, X) - \frac{1}{2}\sqrt{1+x+x^2}\ln(Y) + \sqrt{1+x}\left(\frac{1}{4}\,\ln(T) + \frac{\sqrt{3}}{2}\arctan(U)\right)\right\}, \tag{10a}$$

where X is given by (9b) and the new quantities Y, T, and U are equal to

$$Y = \frac{x(2\sqrt{1+x+x^2} - \sqrt{3}x)}{\sqrt{3}(1+x) + \sqrt{(1+x+x^2)(3+3x+x^2)}}, \tag{10b}$$

$$T = \frac{\sqrt{3+3x+x^2} - \sqrt{3(1+x)}}{\sqrt{3+3x+x^2} + \sqrt{3(1+x)}}, \tag{10c}$$

$$U = \frac{3\sqrt{1+x}}{2x + \sqrt{3+3x+x^2}}. \tag{10d}$$

The behaviour of this ratio is shown in Fig. 2. Some remarkable values are 1.075, 1.048, 1.149 for $x = 0, 1, 20$. The function $R_{G/Y}(x)$ passes through a minimum 1.043

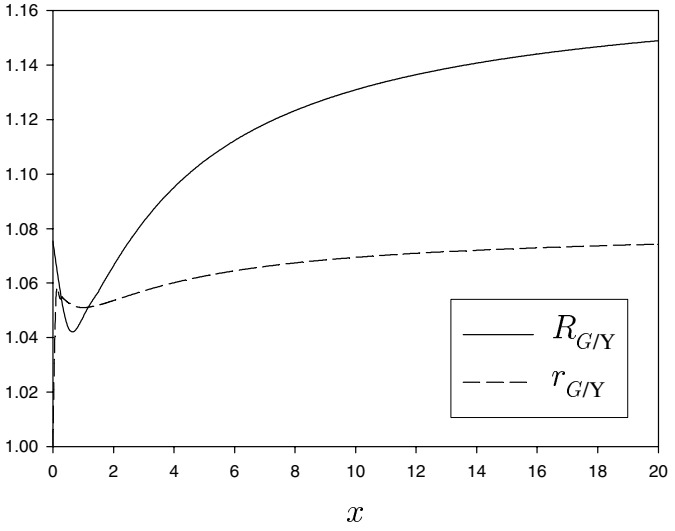

Fig. 2. Ratio $R_{G/Y}(x)$ from the geometrical treatment (see formula (10)) and ratio $r_{G/Y}(x) = b_G(x)/b_Y(x)$ from the hyperspherical treatment (see formulas (34) and (41)), as a function of the mass ratio x

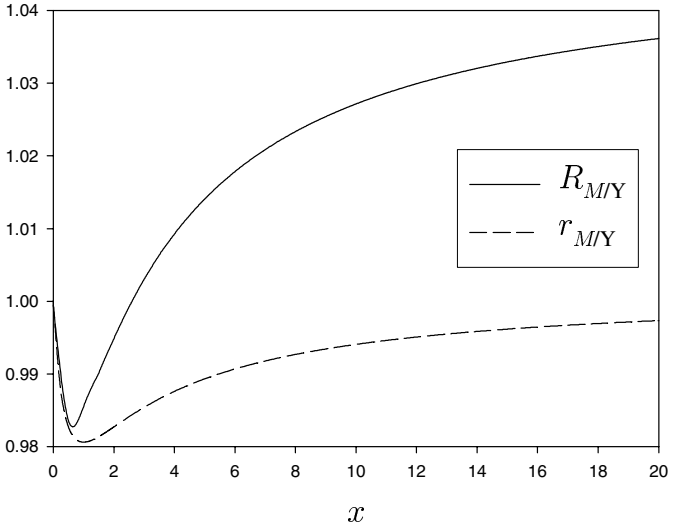

Fig. 3. Ratio $R_{M/Y}(x)$ from the geometrical treatment (see formula (11)) and ratio $r_{M/Y}(x)$ from the hyperspherical treatment (see formula (42)), as a function of the mass ratio x

for $x \approx 0.585$, corresponding again to the Ξ baryon. It is very instructive to remark that for a large domain of mass ratios $0 < x < 5$, the error introduced by replacing the Toricelli point by the centre of mass is less than 10%.

2.6 Another approximation

Replacing the genuine string junction potential by a sum of the two-body confining potentials is a rather good approximation in any case. Replacing it by a sum of one-body centre of mass string potentials is even a better approximation for equal quark mass systems and one light-two heavy quark ones. This approximation becomes slightly worse (although not dramatically) for one heavy–two light quark systems. In most cases, these approximations are better than 10%.

It is interesting to remark that the genuine string tension is *always comprised* between half perimeter and centre of mass junction. This last property is obvious since the Toricelli point is precisely the one which minimises the sum of the distances; in contrast the former property is by no means obvious. One can take benefit of this remark and define a new ratio by

$$R_{M/Y}(x) = \frac{1}{2}\left(R_{C/Y} + R_{G/Y}(x)\right). \tag{11}$$

In (11), the function $R_{G/Y}(x)$ has been computed before. The value of $R_{C/Y}$ can be computed analytically. The result is

$$R_{C/Y} = \frac{1}{6\pi}\Big(3 + \left(1+\sqrt{3}\right)\pi - 3\left[2\ln(2) + \ln\left(\sqrt{3}-1\right) - 3\ln\left(\sqrt{3}+1\right)\right]\Big) \approx 0.923. \tag{12}$$

The curve $R_{M/Y}(x)$ is plotted in Fig. 3. One can remark that the values of $R_{M/Y}(x)$ differ from unity by less than 3% for all relevant values of the x parameter. So this procedure to simulate the genuine string junction potential seems preferable to the previous discussed ones.

3 Hyperspherical approach

3.1 Hyperspherical coordinates

The hyperspherical formalism is an economical way to tackle the three-body problem. We refer to specialised papers for technical aspects (see for instance [9]). Here we just recall what is needed for our purpose.

Let us define a reference mass m and introduce the dimensionless quantities $\omega_i = m_i/m$, $\omega_{ij} = \omega_i + \omega_j$ and $\omega = \omega_1 + \omega_2 + \omega_3$. The first thing to do is to introduce the Jacobi coordinates

$$\boldsymbol{\rho}_{ij} = \alpha_{ij}(\mathbf{r}_i - \mathbf{r}_j), \quad \boldsymbol{\lambda}_{ij} = \beta_{ij}\left(\frac{\omega_i \mathbf{r}_i + \omega_j \mathbf{r}_j}{\omega_{ij}} - \mathbf{r}_k\right), \tag{13}$$

with

$$\alpha_{ij} = \sqrt{\frac{\omega_i\omega_j}{\omega_{ij}}}, \qquad \beta_{ij} = \sqrt{\frac{\omega_k\omega_{ij}}{\omega}},$$
$$\Omega = \alpha_{ij}\beta_{ij} = \sqrt{\frac{\omega_1\omega_2\omega_3}{\omega}}. \tag{14}$$

The normalization quantities have been set in order to obtain nice properties under particle permutations. From now on, we specialise to the 1–2 pair and drop the 12 index everywhere, so that the Jacobi coordinates for our problem are denoted simply $\boldsymbol{\rho}$ (instead of $\boldsymbol{\rho}_{12}$) and $\boldsymbol{\lambda}$ (instead of $\boldsymbol{\lambda}_{12}$).

Each inter-distance $\mathbf{r}_{ij} = \mathbf{r}_i - \mathbf{r}_j$ can be expressed only in terms of $\boldsymbol{\rho}$ and $\boldsymbol{\lambda}$, so that half the perimeter of the quark triangle is expressed as $P(\boldsymbol{\rho}^2, \boldsymbol{\lambda}^2, \boldsymbol{\rho}\cdot\boldsymbol{\lambda})$. The same is true for the positions relative to the centre of mass $\mathbf{s}_i = \mathbf{r}_i - \mathbf{R}_{\rm cm}$, so that the centre of mass string distance is $D(\boldsymbol{\rho}^2, \boldsymbol{\lambda}^2, \boldsymbol{\rho}\cdot\boldsymbol{\lambda})$. Finally, the same property is valid for the genuine string distance $L(\boldsymbol{\rho}^2, \boldsymbol{\lambda}^2, \boldsymbol{\rho}\cdot\boldsymbol{\lambda})$. Over the six original variables defining the configuration, three have disappeared corresponding to the three Euler angles giving the orientation of the plane of the quarks in a fixed reference frame. The confining potential is expressed in terms of two distances ρ and λ, and one angle $\chi = (\widehat{\rho}, \widehat{\lambda})$ between $\boldsymbol{\rho}$ and $\boldsymbol{\lambda}$. Instead of ρ and λ, the hyperspherical formalism introduces the hyperradius R and the hyperangle θ through a polar transformation

$$\rho = R\sin\theta, \quad \lambda = R\cos\theta \quad \text{with} \quad 0 \le \theta \le \pi/2. \tag{15}$$

The hyperradius is invariant under quark permutations

$$R = \sqrt{\rho^2+\lambda^2} = \sqrt{\rho_{23}^2+\lambda_{23}^2} = \sqrt{\rho_{31}^2+\lambda_{31}^2}. \tag{16}$$

The elementary volume element with the hyperspherical coordinates is simply

$$\begin{aligned} \mathrm{d}V &= R^5 \mathrm{d}R \mathrm{d}\Omega^{(6)}, \\ \mathrm{d}\Omega^{(6)} &= \cos^2\theta\, \sin^2\theta\, \mathrm{d}\theta\, \sin\chi\, \mathrm{d}\chi\, \mathrm{d}\Omega^{(3)}, \end{aligned} \tag{17}$$

where $\mathrm{d}\Omega^{(6)}$ is the volume element on the hyperangles and $\mathrm{d}\Omega^{(3)}$ the usual volume element on Euler angles. One has obviously

$$\int \mathrm{d}\Omega^{(3)} = 8\pi^2, \qquad \int \mathrm{d}\Omega^{(6)} = \pi^3. \tag{18}$$

An important property of the hyperspherical formalism is that a dominant part of the interaction comes from the hypercentral approximation of the potential $V(\boldsymbol{\rho}, \boldsymbol{\lambda})$ which is the average of the potential over the hyperangles

$$V(R) = \frac{1}{\pi^3} \int V(\boldsymbol{\rho}, \boldsymbol{\lambda})\, \mathrm{d}\Omega^{(6)}. \tag{19}$$

For potentials invariant under rotations, as the confining term we are interesting in, the expression does not depend on the Euler angles so that, in practice, the hypercentral potential is simply

$$V(R) = \frac{8}{\pi} \int_0^{\pi/2} \cos^2\theta \sin^2\theta \mathrm{d}\theta \int_0^{\pi} V(R,\theta,\chi) \sin\chi \mathrm{d}\chi\,. \tag{20}$$

In the hypercentral approximation the complicated three-body problem reduces to a differential equation including $V(R)$. Within this approximation, we obtain directly an average value of the potential confining energy depending only on the hyperradius. Such a treatment is feasible for the Y-shape as well as its approximants.

In this paper, we focus only on the genuine confining potential V_Y and its two approximations V_C and V_G. In terms of the hyperradius R and hyperangles θ and χ, they are defined by

$$V_Y(R,\theta,\chi) = \sigma L(R,\theta,\chi), \tag{21a}$$

$$V_C(R,\theta,\chi) = \sigma P(R,\theta,\chi), \tag{21b}$$

$$V_G(R,\theta,\chi) = \sigma D(R,\theta,\chi). \tag{21c}$$

The hypercentral approximations of formulas (21) resulting from (20) are denoted here $V_Y(R)$, $V_C(R)$ and $V_G(R)$.

The expressions for P and D are easy to obtain. For the moment, let us quote the following formulas:

$$D(R,\theta,\chi) = \sum_{i<j} \frac{\beta_{ij}}{\omega_k} \lambda_{ij} \tag{22}$$

and

$$P(R,\theta,\chi) = \frac{1}{2} \sum_{i<j} \frac{\rho_{ij}}{\alpha_{ij}}. \tag{23}$$

The expression for L is much more cumbersome. As was mentioned above, there are three special cases for which the angles $\Theta_i = (\widehat{r_{ij}}, \widehat{r_{ik}})$ are greater than 120° ($-1 < \cos\Theta_i < -1/2$); in this case $L = r_{ij} + r_{ik}$. The "normal case" (all Θ_i less than 120°) is $L = r_{\rm I1} + r_{\rm I2} + r_{\rm I3}$ and is less easily obtained. Let us quote the final expression.

(1) First region:

$$-1 < \frac{\frac{\Omega}{\omega_1}\tan\theta + \cos\chi}{\sqrt{\frac{\Omega^2}{\omega_1^2}\tan^2\theta + 2\frac{\Omega}{\omega_1}\tan\theta\cos\chi + 1}} < -\frac{1}{2}, \tag{24}$$

$$\begin{aligned} &L_1(R,\theta,\chi) \\ &= R\cos\theta \left[\frac{\tan\theta}{\alpha} + \frac{1}{\beta}\sqrt{\frac{\Omega^2}{\omega_1^2}\tan^2\theta + 2\frac{\Omega}{\omega_1}\tan\theta\cos\chi + 1} \right]. \end{aligned} \tag{25}$$

(2) Second region:

$$-1 < \frac{\frac{\Omega}{\omega_2}\tan\theta - \cos\chi}{\sqrt{\frac{\Omega^2}{\omega_2^2}\tan^2\theta - 2\frac{\Omega}{\omega_2}\tan\theta\cos\chi + 1}} < -\frac{1}{2}, \tag{26}$$

$$\begin{aligned} &L_2(R,\theta,\chi) \\ &= R\cos\theta \left[\frac{\tan\theta}{\alpha} + \frac{1}{\beta}\sqrt{\frac{\Omega^2}{\omega_2^2}\tan^2\theta - 2\frac{\Omega}{\omega_2}\tan\theta\cos\chi + 1} \right]. \end{aligned} \tag{27}$$

(3) Third region:

$$\begin{aligned} -1 < &\frac{1 + \Omega\left(\frac{1}{\omega_1} - \frac{1}{\omega_2}\right)\tan\theta\cos\chi - \frac{\Omega^2}{\omega_1\omega_2}\tan^2\theta}{\sqrt{1 + 2\frac{\Omega}{\omega_1}\tan\theta\cos\chi + \frac{\Omega^2}{\omega_1^2}\tan^2\theta}\sqrt{1 - 2\frac{\Omega}{\omega_2}\tan\theta\cos\chi + \frac{\Omega^2}{\omega_2^2}\tan^2\theta}} \\ &< -\frac{1}{2}, \end{aligned} \tag{28}$$

$$L_3(R,\theta,\chi) = \frac{R\cos\theta}{\beta} \left[\sqrt{1 + 2\frac{\Omega}{\omega_1}\tan\theta\cos\chi + \frac{\Omega^2}{\omega_1^2}\tan^2\theta} \right.$$

$$+\sqrt{1-2\frac{\Omega}{\omega_2}\tan\theta\cos\chi+\frac{\Omega^2}{\omega_2^2}\tan^2\theta}\Bigg]. \quad (29)$$

(4) Fourth region or "normal region":

$$-1/2<\cos\Theta_i<1 \quad \forall\, i, \quad (30)$$

$$L_4(R,\theta,\chi)=R\cos\theta \times\left\{\frac{\omega_1^3-\omega_2^3}{\omega_1\omega_2(\omega_1^2-\omega_2^2)}\tan^2\theta+\left[\frac{\omega_2-\omega_1}{\omega_{12}}\cos\chi+\sqrt{3}\sin\chi\right]\frac{\tan\theta}{\Omega}+\frac{1}{\beta^2}\right\}^{1/2}. \quad (31)$$

Since each distance is proportional to the hyperradius, all the confining potentials under consideration have the form $(I=C,G,Y)$

$$V_I(R)=b_I(\omega_1,\omega_2,\omega_3)R. \quad (32)$$

One sees that in the hyperspherical formalism the confining potential remains linear, with a string tension which is no longer σ but a modified value b which depends on the system. This dependence is not of a geometrical nature, as in the previous section for V_G, but of a dynamical character that comes from the choice of the Jacobi coordinates. The main effort of this section is devoted to the calculation of this new "string" tension b.

To stick to the previous section and also to get analytical results, we restrict ourselves from now on to the case of two identical particles (particles 1 and 2 with the reference mass $m=m_1=m_2$ and a particle 3 with mass $m_3=xm$). In this special case, the coefficients α and β in (14) are

$$\alpha=\frac{1}{\sqrt{2}},\quad \beta=\sqrt{\frac{2x}{2+x}},\quad \Omega=\alpha\beta=\sqrt{\frac{x}{2+x}}. \quad (33)$$

Let us study separately each approximation.

3.2 Centre of mass junction

Among the three contributions to the potential (22), one is particularly simple. It corresponds to $s_3=(\beta R\cos\theta)/\omega_3$. The averaging is trivial and gives the value $32\beta R/(15\pi\omega_3)$. The calculation of s_1 is longer but presents no special difficulty. A trick to get the answer is to remark that R is an invariant under quark permutations. Consequently, the averaging can be performed with the hyperspherical angles θ_{23} and χ_{23} as well, so that the result follows immediately from the previous one giving the contribution $32\beta_{23}R/(15\pi\omega_1)$. Similarly the contribution due to s_2 is $32\beta_{31}R/(15\pi\omega_2)$. Replacing the quantities β_{ij},ω_k by their values (33) gives the final result for the effective string tension in this approximation,

$$b_G(x)=\frac{32}{15\pi}\sigma\left[\sqrt{\frac{2}{x(2+x)}}+2\sqrt{\frac{1+x}{2+x}}\right]. \quad (34)$$

3.3 Half the perimeter

The procedure is essentially the same using now the potential (23). The contribution due to $r_{12}=\rho/\alpha$ is very easy to obtain; the result is $32R/(15\pi\alpha)$. Switching to the permuted hyperangles immediately gives the contributions due to r_{23} and r_{31}, namely $32R/(15\pi\alpha_{23})$ and $32R/(15\pi\alpha_{31})$ respectively. Replacing the quantities α_{ij} by their values (33) gives the final result for the effective string tension in this approximation

$$b_C(x)=\frac{32}{15\pi}\sigma\left[\frac{1}{\sqrt{2}}+\sqrt{\frac{1+x}{x}}\right]. \quad (35)$$

3.4 Genuine string junction

Because of the special cases, several zones of the plane (θ,χ) must be isolated corresponding to the conditions ((24), (26) and (28)), where the integrand has a special form ((25), (27) and (29)). These various zones are separated from the "normal zone" by a line which corresponds to the limit $\cos\Theta_i=-1/2$. It is convenient to take θ as abscissa and χ as ordinate in the plane.

The condition (24) is explicitly written

$$\chi_1(\theta)=\arccos\left[\frac{-3\Omega\tan\theta-\sqrt{4-3\Omega^2\tan^2\theta}}{4}\right]. \quad (36)$$

This curve starts with the value $2\pi/3$ for $\theta=0$ and ends up at π for $\theta=\theta_0=\arctan(1/\Omega)$. In the first region, above χ_1, the expression $L=L_1$ (25) applies.

The condition (26) explicitly reads

$$\chi_2(\theta)=\arccos\left[\frac{3\Omega\tan\theta+\sqrt{4-3\Omega^2\tan^2\theta}}{4}\right]=\pi-\chi_1(\theta). \quad (37)$$

This curve starts with the value $\pi/3$ for $\theta=0$ and ends up at 0 for $\theta=\theta_0$. In the second region, below χ_2, the expression $L=L_2$ (27) applies.

Finally a third region is found from condition (28), which explicitly reads in terms of two functions

$$\chi_3^-(\theta)=\arccos\left[\frac{\sqrt{(3\Omega^2\tan^2\theta-1)(3-\Omega^2\tan^2\theta)}}{2\Omega\tan\theta}\right],$$
$$\chi_3^+(\theta)=\pi-\chi_3^-(\theta). \quad (38)$$

These curves start with the values 0 and π for $\theta=\theta_0$ and join at the common value $\pi/2$ for $\theta=\theta_1=\arctan(\sqrt{3}/\Omega)$. In the third region, at the right of χ_3, the expression $L=L_3$ (29) applies.

In the rest of the plane, the "normal" expression L_4 (31) is valid. The situation is summarised in Fig. 4.

To obtain $b_Y(x)$ we integrate the function $L(R,\theta,\chi)$ in the plane θ,χ. The result is given as the sum of seven contributions:

$$I=\frac{1}{\pi^3}\int L(R,\theta,\chi)\,\mathrm{d}\Omega^{(6)}$$

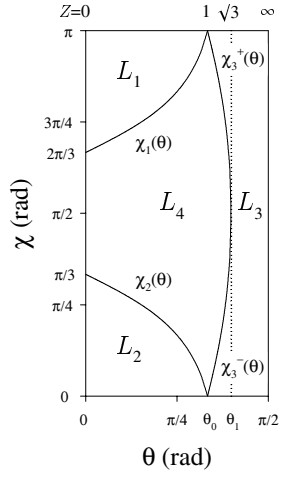

Fig. 4. Integration domain of quantity $L(R,\theta,\chi)$ as a function of angles θ and χ (see Sect. 3.1)

$$= \frac{8\alpha R}{\pi}\left(I_1+I_2+I_3+I_4+I_5+I_6+I_7\right). \quad (39)$$

We were not able to obtain an analytical formula for I. The best that we can do is to transform the double integral into a single integral noting that the integrals over χ can be calculated analytically. Instead of integration over θ, it is much simpler to perform the change of variable $Z = \Omega\tan\theta$. With these options, one has explicitly

$$I_1 = \Omega^3\int_0^1 \frac{Z^2\,\mathrm{d}Z}{\left(Z^2+\Omega^2\right)^{7/2}} \quad (40a)$$
$$\times\int_0^{\chi_2(Z)}\left[2Z+\sqrt{1+Z^2-2Z\cos\chi}\right]\sin\chi\,\mathrm{d}\chi,$$

$$I_2 = \Omega^3\int_0^1 \frac{Z^2\,\mathrm{d}Z}{\left(Z^2+\Omega^2\right)^{7/2}} \quad (40b)$$
$$\times\int_{\chi_2(Z)}^{\chi_1(Z)}\left[\sqrt{1+3Z^2+2\sqrt{3}Z\sin\chi}\right]\sin\chi\,\mathrm{d}\chi,$$

$$I_3 = \Omega^3\int_0^1 \frac{Z^2\,\mathrm{d}Z}{\left(Z^2+\Omega^2\right)^{7/2}} \quad (40c)$$
$$\times\int_{\chi_1(Z)}^{\pi}\left[2Z+\sqrt{1+Z^2+2Z\cos\chi}\right]\sin\chi\,\mathrm{d}\chi,$$

$$I_4 = \Omega^3\int_1^{\sqrt{3}} \frac{Z^2\,\mathrm{d}Z}{\left(Z^2+\Omega^2\right)^{7/2}} \quad (40d)$$
$$\times\int_0^{\chi_3^-(Z)}\left[\sqrt{1+Z^2+2Z\cos\chi}+\sqrt{1+Z^2-2Z\cos\chi}\right]\sin\chi\,\mathrm{d}\chi,$$

$$I_5 = \Omega^3\int_1^{\sqrt{3}} \frac{Z^2\,\mathrm{d}Z}{\left(Z^2+\Omega^2\right)^{7/2}} \quad (40e)$$
$$\times\int_{\chi_3^-(Z)}^{\chi_3^+(Z)}\left[\sqrt{1+3Z^2+2\sqrt{3}Z\sin\chi}\right]\sin\chi\,\mathrm{d}\chi,$$

$$I_6 = \Omega^3\int_1^{\sqrt{3}} \frac{Z^2\,\mathrm{d}Z}{\left(Z^2+\Omega^2\right)^{7/2}} \quad (40f)$$
$$\times\int_{\chi_3^+(Z)}^{\pi}\left[\sqrt{1+Z^2+2Z\cos\chi}+\sqrt{1+Z^2-2Z\cos\chi}\right]\sin\chi\,\mathrm{d}\chi,$$

$$I_7 = \Omega^3\int_{\sqrt{3}}^{\infty} \frac{Z^2\,\mathrm{d}Z}{\left(Z^2+\Omega^2\right)^{7/2}} \quad (40g)$$
$$\times\int_0^{\pi}\left[\sqrt{1+Z^2+2Z\cos\chi}+\sqrt{1+Z^2-2Z\cos\chi}\right]\sin\chi\,\mathrm{d}\chi.$$

Due to the symmetries of the problem, it is easy to show that $I_1 = I_3$ and $I_4 = I_6$. The integrals I_1, I_4, I_7 can be calculated analytically, but not I_2 and I_5.

The calculation is not trivial, but some help is provided by the Mathematica package. One obtains

$$b_Y(x) = \frac{32\sigma}{15\pi}\sqrt{2}\left\{\frac{28+39\Omega^2+18\Omega^4}{4\left(4+3\Omega^2\right)^2}\right.$$
$$+\frac{120+368\Omega^2+612\Omega^4+641\Omega^6+377\Omega^8+105\Omega^{10}+9\Omega^{12}}{2\Omega\left(4+3\Omega^2\right)^2\left(3+\Omega^2\right)^2\left(1+\Omega^2\right)^{3/2}}$$
$$+\frac{5\Omega^3}{4\sqrt{3}}\int_0^1\frac{\mathrm{d}Z\,Z\left(1+\sqrt{3}Z\right)}{\left(Z^2+\Omega^2\right)^{7/2}}$$
$$\times\left[\left(1+3Z^2\right)E\left(\frac{\pi}{4}-\frac{\chi_2}{2},u\right)\right.$$
$$\left.-\left(1-\sqrt{3}Z\right)^2F\left(\frac{\pi}{4}-\frac{\chi_2}{2},u\right)\right]$$
$$+\frac{5\Omega^3}{4\sqrt{3}}\int_1^{\sqrt{3}}\frac{\mathrm{d}Z\,Z\left(1+\sqrt{3}Z\right)}{\left(Z^2+\Omega^2\right)^{7/2}}$$
$$\times\left[\left(1+3Z^2\right)E\left(\frac{\pi}{4}-\frac{\chi_3^-}{2},u\right)\right.$$
$$\left.\left.-\left(1-\sqrt{3}Z\right)^2F\left(\frac{\pi}{4}-\frac{\chi_3^-}{2},u\right)\right]\right\}, \quad (41a)$$

with

$$\Omega(x) = \sqrt{\frac{x}{2+x}}, \quad u(Z) = \frac{4\sqrt{3}Z}{\left(1+\sqrt{3}Z\right)^2},$$
$$\chi_2(Z) = \arccos\left[\frac{3Z+\sqrt{4-3Z^2}}{4}\right],$$
$$\chi_3^-(Z) = \arcsin\left[\frac{\sqrt{3}\left(Z^2-1\right)}{2Z}\right], \quad (41b)$$

and $F(\phi, m)$ and $E(\phi, m)$ are respectively the elliptic integrals of the first and second kinds [17].

3.5 Comparison of the effective string tensions

It is interesting to compare the string tensions $b_G(x)$ (34), $b_C(x)$ (35), $b_Y(x)$ (41) for the three expressions of the confining operator. Contrary to the previous geometrical approach they all depend on the system; as in the preceding section we introduce the ratios of the string tensions $r_{Y/C}(x) = b_Y(x)/b_C(x)$, $r_{G/C}(x) = b_G(x)/b_C(x)$, $r_{G/Y}(x) = b_G(x)/b_Y(x)$.

3.5.1 Genuine to perimeter

The ratio $r_{Y/C}(x)$ is presented in Fig. 5. It is always greater than 1, indicating that the genuine tension is more repulsive than the two-body approximation. It starts from 1 for $x = 0$, increases to a maximum 1.099 for $x \approx 1$ and then decreases slowly around 1.085 for large values of x. Those values are very close to the constant value 1.086 obtained in the geometrical approach.

3.5.2 Centre of mass to perimeter

The ratio $r_{G/C}(x)$ is plotted in Fig. 1. It starts from 1 for $x = 0$, increases rapidly up to 1.15 for $x \approx 0.5$ and then presents a plateau at this value around $x \approx 1$; it tends asymptotically to $2\sqrt{2}/(1+\sqrt{2}) \approx 1.1715$ for an infinite value of x. Although the forms of the curves for the hyperspherical formalism and the geometrical approach are not identical, the values for the corresponding ratios are rather close.

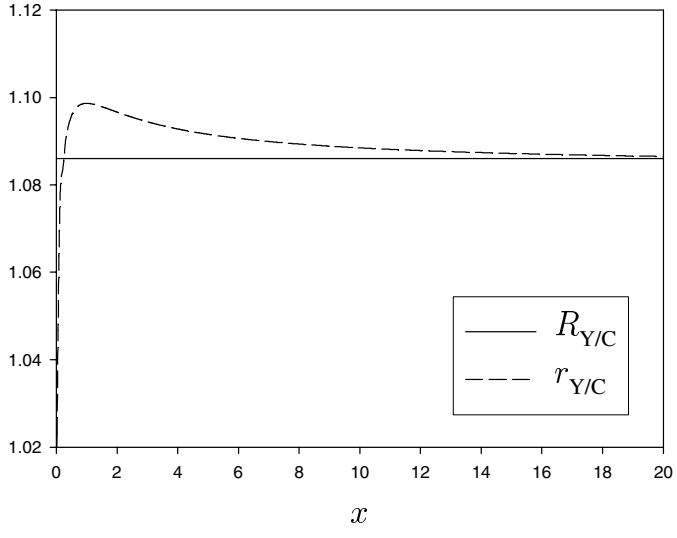

Fig. 5. Ratio $R_{Y/C} \approx 1.086$ from the geometrical treatment (see formula (8)) and ratio $r_{Y/C}(x) = b_Y(x)/b_C(x)$ from the hyperspherical treatment (see formulas (41) and (35)), as a function of the mass ratio x

3.5.3 Centre of mass to genuine

The ratio $r_{G/Y}(x)$ is shown in Fig. 2. It starts from 1 for $x = 0$, rises to the local maximum of 1.0556 for $x \approx 0.195$, then passes through the local minimum of 1.051 for $x \approx 1$ and rises very slowly to 1.08 for large values of x. Here again the values are in nice agreement with the geometrical approach, and are even closer to the genuine case.

3.5.4 Another approximation

In the hyperspherical formalism, we find the same features concerning the approximations as in the geometrical approach: for a given value of the string constant σ, the centre of mass junction potential is more repulsive than the potential with the genuine junction which is in turn more repulsive than half the perimeter potential. These two approximations can be considered as quite reasonable, differing by no more than 10% as compared to the genuine string junction one.

As in the case of the geometrical approach, one may notice that $b_Y(x)$ is always comprised between $b_C(x)$ and $b_G(x)$. Thus it is tempting to define a new approximation $b_M(x)$ and a new ratio $r_{M/Y}(x)$ similar to that of (11) by

$$r_{M/Y}(x) = \frac{b_M(x)}{b_Y(x)} = \frac{(b_C(x) + b_G(x))/2}{b_Y(x)} = \frac{1}{2}\left(r_{C/Y}(x) + r_{G/Y}(x)\right). \quad (42)$$

The curve $r_{M/Y}(x)$ is plotted in Fig. 3. One can remark from this figure that $r_{M/Y}(x)$ differs from unity by less than 2% for all values of the parameter x. Like in the geometrical case, using this prescription to simulate the genuine string junction potential seems more preferable than the ones discussed previously.

4 Three-body calculations

4.1 Strategy

For a system composed of two identical particles of mass m and a third particle of mass $M = xm$, the three-body equation in the hypercentral approximation to the hyperspherical formalism is very simple; it looks like

$$[K(x, R) + b(x)R]\Psi(R) = E\Psi(R). \quad (43)$$

In this expression E is the energy eigenvalue, and $K(x, R)$ symbolises the differential operator corresponding to the kinetic energy plus all the hypercentral potentials except the confining hypercentral interaction which is explicitly written as $b(x)R$, as it was proved in the preceding section. Up to now, we considered three types of confining potentials V_I, labelled by an index I ($I = Y$ for the genuine three-body confinement, $I = C$ for the two-body half perimeter confinement and $I = G$ for the one-body centre

of mass junction). The important point is that, for these three possibilities, the operator $K(x, R)$ is *the same*. For a given string tension σ, the only difference lies in a different value of the constant $b(x)$ appearing in (43). For a genuine string tension, we have the value $b(x) = b_Y(x)$ given by (41), while for centre of mass junction and half perimeter confinement one must employ the $b_G(x)$ and $b_C(x)$ of formulas (34) and (35) respectively. The numerical results of the various possibilities are of course different although they should be close, within less than 10%. This property was the conclusion of our two previous sections.

In the light of the behaviour of the curves $R_{M/Y}(x)$ and $r_{M/Y}(x)$, it is natural to try to simulate the potential V_Y by defining a new confining potential

$$V_M = \frac{1}{2}\,(V_C + V_G)\,, \tag{44}$$

with V_C and V_G given respectively by formulas (2) and (3). Let us emphasise that the unique above definition agrees with both the geometrical approach for the ratio $R_{M/Y} = V_M/V_Y$ and the hyperspherical approach using $b_M(x)$.

As the ratios $R_{M/Y}(x)$ and $r_{M/Y}(x)$ are very close to 1, one can hope that the V_M and the V_Y will give similar spectra with the same string tension. The situation is not so favourable for potentials V_C and V_G since the corresponding ratios R and r may differ from 1 by more than 10%. Nevertheless, we can try to simulate results obtained from the Y-shape potential by using a renormalised value of the string tension in potentials V_C and V_G.

Indeed, let us suppose that we perform an hyperspherical calculation for the I approximation with a string constant σ_I. Now let us perform an hyperspherical calculation for the J approximation, not with an identical string constant $\sigma_J = \sigma_I$, but with a string constant modified in the following way:

$$\sigma_J(x) = \sigma_I\, r_{I/J}(x) \qquad (\sigma_J(x) = \sigma_I\, b_I(x)/b_J(x))\,.$$

Obviously, one recovers the original equation and thus the original results. In other words, one can simulate the results of a treatment based on the approximation I, by performing a treatment based on the approximation J, provided we change the string constant in a consistent way. This conclusion is perfectly exact for the hypercentral approximation. This does not mean that it must remain exact if we perform a more sophisticated three-body treatment. The quality of this simulation, as well as the results coming from V_M, are the subjects of this section.

Our numerical algorithm to solve the three-body problem with potentials V_C, V_G and V_M is based on an expansion of the wave function in terms of harmonic oscillator functions with different sizes [18]. It was checked with other methods and was proved to give results of good accuracy if the expansion is pushed sufficiently far (let say up to 16–20 quanta). Moreover, it can deal easily with a relativistic kinetic energy operator. The details of technical aspects are not the subject of this paper and can be found elsewhere [19]. For the present purposes, it is enough to say that we are able to solve in a very fast and precise way a three-body calculation either with a non-relativistic or relativistic expression for the kinetic energy operator.

One-body and two-body operators are easy to implement, but three-body operators are much more complicated to handle, specially if one must distinguish several integration domains, as it is the case for the Y-shape potential. In this paper, the three-body problem with potentials V_Y is solved by the hyperspherical method without the limitation of the hypercentral approximation [9]. At the present stage, only S-wave states can be computed with a good accuracy. This is why the simulation of a three-body operator either with a two-body, a one-body operator, or a mixing of both is important.

We consider a system composed of three quarks of type n (for u or d), s, c, b. In this paper, we are only interested in the possibility to simulate the genuine confinement by simpler potentials and, for that purpose, it is enough to restrict the interaction to the confining term only. Forgetting about Coulomb, hyperfine and constant potentials, our results cannot be compared to physical systems. But the comparison of the various simulations between themselves is very instructive. Just to have some connections with real systems, we put arbitrarily the masses of the quarks at the physical values (in GeV) [11]: $m_n = 0.330$, $m_s = 0.550$, $m_c = 1.850$, $m_b = 5.200$. The only potential taken into account is the linear confining potential as defined in the first section. To see the sensitivity of the results versus the kinematics, we perform two types of calculation: one based on a non-relativistic expression (Schrödinger equation), and one based on a relativistic expression (spinless Salpeter equation). To test also the sensitivity to excited states, we performed the calculations not only for ground states ($L = 0$ and $N = 1$), but also for the first radial excited state ($L = 0$ and $N = 2$), and when it is possible the first orbital excited state ($L = 1$ and $N = 1$).

4.2 Comparison centre of mass to perimeter

This section does not deal with the Y-shape potential, but nevertheless it is important because we compare here two treatments that we are able to handle easily, in any physical situation, and with a good accuracy. The possibility to simulate one treatment by the other is very instructive and can be tested carefully, so that firm conclusions can be drawn.

For a number of systems, exploring a large domain of the x parameter, we calculate first the baryon binding energies obtained with the centre of mass junction (G approximation) and with the half perimeter confinement (C approximation) using the same value of the string tension $\sigma = 0.2\,\mathrm{GeV}^2$. This value is close to the accepted value coming from lattice calculations [1]. Then we keep this value of σ, do the calculations for the G approximation using a modified value of the string tension based on the arguments of the geometrical approach $\sigma_R(x) = \sigma\, R_{C/G}(x)$ and on the arguments of the hyperspherical approach $\sigma_r(x) = \sigma\, r_{C/G}(x)$ and compare with the C calculation with the string tension at the value σ. We also perform the recip-

Table 1. Simulation of interaction V_C by interaction V_G, and vice versa, for non-relativistic kinematics. Binding energy in GeV of various baryons as a function of the total orbital angular momentum L, the total angular momentum and parity J^P, the principal quantum number N, the type of confinement potential (Conf.), and the value of the string junction σ in GeV^2. The total spin is equal to J and the total isospin is the lowest one. The mass ratio x is also given for each system. Data columns are numbered to make the discussion easier

System	L	J^P	N	Conf.	V_C	V_G	V_G	V_G	V_C	V_C
				σ	0.2	$0.2 r_{C/G}$	$0.2/R_{G/C}$	0.2	$0.2\, r_{G/C}$	$0.2\, R_{G/C}$
					(1)	(2)	(3)	(4)	(5)	(6)
nnn	0	$1/2^+$	1		1.912	1.912	1.933	2.104	2.104	2.081
($x = 1$)			2		2.633	2.633	2.662	2.898	2.898	2.867
	1	$1/2^-$	1		2.332	2.332	2.358	2.567	2.567	2.539
bbb	0	$3/2^+$	1		0.763	0.763	0.771	0.839	0.839	0.830
($x = 1$)			2		1.050	1.050	1.062	1.156	1.156	1.143
	1	$1/2^-$	1		0.930	0.930	0.940	1.024	1.024	1.013
snn	0	$1/2^+$	1		1.819	1.821	1.827	2.004	2.002	1.996
($x = 1.667$)			2		2.480	2.505	2.513	2.758	2.730	2.721
	1	$1/2^-$	1		2.192	2.214	2.221	2.437	2.413	2.405
bnn	0	$1/2^+$	1		1.652	1.673	1.604	1.854	1.831	1.909
($x = 15.76$)			2		2.171	2.300	2.205	2.548	2.405	2.509
	1	$1/2^-$	1		1.939	2.037	1.953	2.256	2.149	2.241
nss	0	$1/2^+$	1		1.719	1.721	1.744	1.894	1.891	1.866
($x = 0.6$)			2		2.335	2.359	2.390	2.595	2.569	2.536
	1	$1/2^-$	1		2.067	2.086	2.114	2.296	2.275	2.245
nbb	0	$1/2^+$	1		1.247	1.278	1.246	1.373	1.339	1.374
($x = 0.063$)			2		1.514	1.599	1.559	1.718	1.626	1.668
	1	$1/2^-$	1		1.397	1.465	1.428	1.574	1.501	1.540

rocal calculations. Our quantitative results are presented in Table 1 for non-relativistic kinematics.

Note that the definition of the ratio $r_{I/J}$ (see Sect. 3.5) implies that $r_{J/I} = 1/r_{I/J}$. This property is not exact for the ratio $R_{I/J}$. However, the value $1/R_{C/Y} \approx 1.083$ (coming from (12)) must be compared with $R_{Y/C} \approx 1.086$ (see (8)). These values are very close and this gives us confidence in the use of $R_{J/I} \approx 1/R_{I/J}$ for all cases.

If we compare column (1) and column (4) from Table 1, we can see that, with the same string tension, masses obtained by potentials V_C or V_G are rather different. The binding energy can differ by about 200 MeV or more. So it is relevant to answer the question: "Is it possible to simulate each potential by the other, simply in adjusting the value of the string tension?".

If we look at columns (1) and (2) for systems characterised by $x = 1$, we can see that all masses are identical (actually, they differ at the 6th digit, which is at the limit of the accuracy of our calculation method). It is then possible to simulate perfectly the potential V_C with a string tension σ by the potential V_G with the string tension $\sigma\, r_{C/G}$. This property, which is exact at the hypercentral approximation, is also verified for the full calculation for symmetrical systems. The situation is less favourable for systems with $x \neq 1$. In these cases, we can remark that the masses of column (2) are always greater than the masses of column (1). For snn and nss baryons, the agreement is good, especially for the ground state. But for very asymmetrical systems such as bnn and nbb baryons, there can exist greater mass differences, up to about 100 MeV. Let us remark that, for the ground state, the agreement is still reasonable (better than 2%).

If we compare now data from columns (1) and (3), we can see that, in general, the potential V_C is not so well simulated by the potential V_G using $R_{C/G}$ instead of $r_{C/G}$. In particular, masses from these two columns are not identical for systems with $x = 1$ (since an exact simulation is impossible with the geometrical approach, we consider that using $1/R_{C/G}$ instead of $R_{G/C}$ in column (6) do not spoil our conclusions). In most cases, masses of columns (3) are greater than masses of column (2). But for very asymmetrical systems, a peculiar mass in column (3) can be closer to the one in column (1) than the corresponding mass in column (2).

We retrieve the same features in comparing data from columns (4) with data from columns (5) and (6). But one can remark that the masses of column (5) are always smaller than the masses of column (4), when they are not identical. Moreover the masses of column (6) are generally smaller than those of column (5). This situation is the opposite of the one for columns (1), (2) and (3)

Some calculations have also been performed with relativistic kinematics, but the same conclusions can be drawn. We have just remarked that the agreement between the

Table 2. Comparison between genuine potential V_Y with a constant string tension σ, the confining potential V_M with the same string tension, and the V_C and V_G confining interactions with renormalised string tension (see text). Binding energies are obtained for non-relativistic kinematics. Same kind of data as in Table 1

System	L	J^P	N	Conf.	V_Y	V_M	V_C	V_G	V_C	V_G
				σ	0.2	0.2	$0.2\,r_{Y/C}$	$0.2\,r_{Y/G}$	$0.2\,R_{Y/C}$	$0.2/R_{G/Y}$
					(1)	(2)	(3)	(4)	(5)	(6)
nnn	0	$1/2^+$	1		2.032	2.009	2.036	2.036	2.020	2.040
$(x=1)$			2		2.785	2.768	2.804	2.804	2.782	2.810
	1	$1/2^-$	1			2.451	2.483	2.483	2.464	2.488
bbb	0	$3/2^+$	1		0.810	0.801	0.812	0.812	0.806	0.814
$(x=1)$			2		1.111	1.104	1.118	1.118	1.110	1.121
	1	$1/2^-$	1			0.978	0.990	0.990	0.983	0.993
snn	0	$1/2^+$	1		1.933	1.913	1.935	1.937	1.921	1.928
$(x=1.667)$			2		2.626	2.625	2.639	2.666	2.620	2.653
	1	$1/2^-$	1			2.317	2.332	2.356	2.316	2.345
bnn	0	$1/2^+$	1		1.752	1.760	1.747	1.769	1.745	1.695
$(x=15.76)$			2		2.310	2.390	2.295	2.432	2.293	2.330
	1	$1/2^-$	1			2.110	2.050	2.153	2.049	2.063
nss	0	$1/2^+$	1		1.826	1.807	1.828	1.831	1.815	1.841
$(x=0.6)$			2		2.474	2.468	2.484	2.509	2.467	2.523
	1	$1/2^-$	1			2.183	2.199	2.219	2.184	2.231
nbb	0	$1/2^+$	1		1.313	1.312	1.296	1.329	1.317	1.316
$(x=0.063)$			2		1.645	1.618	1.574	1.662	1.599	1.647
	1	$1/2^-$	1			1.488	1.453	1.523	1.476	1.509

masses is slightly less good than in the non-relativistic case. To be complete, let us mention that, with this kinematics, for systems with $x = 1$, the differences between masses computed with V_C (V_G) and those computed with V_G (V_C) and the string tension multiplied by $r_{C/G}$ ($r_{G/C}$) appear at the 5th digit, which can be considered as relevant for the accuracy of our method.

The simulation based on the renormalised string constant originating from the hyperspherical formalism gives generally good results, better than those coming from the geometrical approach. Nevertheless, for very asymmetrical systems, better results can be obtained with this last method.

It is important to emphasise that using renormalised string tensions provides, in any case, much better results (6% in the worst case) than keeping a single value of σ (17% in the worst case, 10% in the best). This study gives strong confidence in the use also of a renormalised σ to simulate the genuine string junction.

4.3 Simulation of the genuine junction

We consider the genuine confining three-body potential with a constant string tension σ and its various approximations. Our quantitative results are presented in Table 2 for non-relativistic kinematics.

In this paper, the spectra of the potential V_Y are obtained by a hyperspherical formalism containing the grand momenta $K = 0, 2, 4$. For the moment, only binding energies of S-wave states have been computed. They are reported in column (1) and are used as a reference to test the quality of the various approximations. All other values have been computed with a harmonic oscillator basis up to 20 quanta. The accuracy of all binding energies is better than 1%.

In column (2), binding energies of the potential V_M are presented. They are obtained with a value for the string tension which is the same as the one used for V_Y. One can see that the numbers of columns (1) and (2) differ generally by less than 20 MeV, with as the only notable exception the first excited S-wave state of the bnn system. We cannot say anything about the P-wave states, but we can expect that the results from the V_M potential are also close to those of the V_Y interaction. Thus, it appears that the potential mixing equally the half perimeter and the centre of mass junction simulates quite well the genuine Y-shape interaction.

Let us now discuss the quality of the spectra obtained with V_C and V_G and with a renormalised string tension as explained previously. We performed the calculation with a two-body confining potential of type C and with a string constant either $\sigma_r^{(C)}(x) = \sigma\, r_{Y/C}(x)$ (column (3)) or $\sigma_R^{(C)} = \sigma\, R_{Y/C}$ (column (5)). Then we redo the calculation with a one-body confining potential of type G and with a string constant of either $\sigma_r^{(G)}(x) = \sigma\, r_{Y/G}(x)$ (column (4)) or $\sigma_R^{(G)}(x) = \sigma\, R_{Y/G}(x)$ (column (6)).

By comparing the data from columns (3) and (4) in Table 2, we can see that the masses for baryons nnn and

bbb are practically the same (differences are at the level of the 6th digit as described in the previous section) and very close to the value of column (1). This means that, for this kind of symmetrical systems, the simulation of the potential V_Y by interactions V_C and V_G, based on the hyperspherical formalism, gives very good results. The situation is less favourable for asymmetrical systems. For *snn* and *nss* baryons, the agreement between columns (3) and (4) is still good, especially for the ground state. But for very asymmetrical systems such as *bnn* and *nbb* baryons, there can exist greater mass differences, up to about 100 MeV. Again, for the ground state, the agreement is still reasonable. Let us remark that the masses in column (4) are always greater than the corresponding ones in column (3). The values of these two columns are in reasonable agreement with the reference results of column (1).

Within the geometrical approach, the results of the two procedures of simulation are never in perfect agreement, as we can see by comparing columns (5) and (6), but the values obtained generally enclose the value of column (1). Let us note that the differences between a mass in column (5) and the corresponding one in column (6) are generally of the same order as the gap between values of columns (3) and (4).

The renormalization of the string tension as suggested by the geometrical and the hyperspherical formalisms allows one to compute with potentials V_C and V_G binding energies which are close to the ones obtained with the potential V_Y. It gives in any case much better results than the ones obtained keeping a fixed value of the string tension.

To be complete, it is worth mentioning that the same conclusions can be obtained with a relativistic kinematics, although in this case we cannot compute the reference energies corresponding to the potential V_Y.

4.4 Particles with different masses

Up to now, the analysis has been done for at least two identical particles. General analytical formulas in the case of three different particles are not available, except b_G and b_C in the hyperspherical formalism. In this case, we noted that the tensions are expressed by

$$b_G = \frac{32}{15\pi}\sigma \sum_{i<j} \frac{\beta_{ij}}{\omega_k}, \tag{45}$$

$$b_C = \frac{32}{15\pi}\sigma \sum_{i<j} \frac{1}{2\alpha_{ij}}. \tag{46}$$

A first possibility to treat easily the problem of three different masses is to use the hypercentral approximation with $b_M = (b_C + b_G)/2$, with the above expressions for b_C and b_G. This procedure would avoid a double numerical integration to get b_Y, whereas allowing results to be obtained of better than 2%.

Another possibility relies on the V_M potential proposed in the previous section. We have verified that this approximation works well in the case of two or three identical particles. We can reasonably assume that it will also be good in the case of three different masses.

5 Conclusion

In this paper, we studied three approximations of the genuine three-body confinement: a two-body potential V_C equal to half perimeter of the triangle formed by the three particles, a one-body potential V_G with the junction point at the centre of mass, and a mixing of both $V_M = (V_C + V_G)/2$. Two approaches were investigated to test the quality of these approximations: a geometrical one for which the important quantities are the various distances in the plane of the particles, and another one based on the hyperspherical formalism. Both give very similar and consistent conclusions. The potential energy V_G overestimates the potential energy of the genuine junction by about 5% in most cases, and about 10% in extreme asymmetrical situations. The confining potential energy V_C underestimates the potential energy of the genuine junction by about 8%. Keeping the same value of the string tension in approximants can induce a 100 MeV error in the calculated masses, as compared to the spectra obtained from the Y-shape confinement. In this respect, the V_M interaction simulates the potential energy of the Y-shape interaction to better than 2%.

Thus, using V_M with the same string tension as the genuine junction gives very good results at the level of the spectra. To obtain a similar quality (sometimes a bit better or a bit worse) for the potentials V_C and V_G, it is necessary to renormalise the string tension by a mass dependent factor that can be analytically computed in the cases of two and three identical particles. This is very important to simplify the technical effort.

Acknowledgements. The authors are grateful to NATO services which give us the possibility to make visits which greatly facilitated this work, through the NATO grant PST.CLG.978710. B. Silvestre-Brac and C. Semay (FNRS Research Associate position) would like to thank the CNRS/CGRI-FNRS agreement for financial support.

References

1. T.T. Takahashi, H. Matsufuru, Y. Nemoto, H. Suganuma, Phys. Rev. Lett. **86**, 18 (2001); Phys. Rev D **65**, 114509 (2002)
2. Y. Koma, E.-M. Ilgenfritz, T. Suzuki, H. Toki, Phys. Rev. D **64**, 014015 (2001)
3. X. Artru, Nucl. Phys. B **85**, 442 (1975)
4. H.G. Dosch, V. Mueller, Nucl. Phys. B **116**, 470 (1976)
5. S. Capstick, N. Isgur, Phys. Rev. D **34**, 2809 (1986)
6. W.H. Blask, U. Bohn, M.G. Huber, B. Ch. Metsch, H.R. Petry, Z. Phys. A **337**, 327 (1990)
7. J. Carlson, J. Kogut, W.R. Pandharipande, Phys. Rev. D **27**, 233 (1983)
8. R. Sartor, F. Stancu, Phys. Rev. D **31**, 128 (1985); D **33**, 727 (1986)
9. M. Fabre de la Ripelle, Yu.A. Simonov, Ann. Phys. (N.Y.) **212**, 235 (1991)
10. T.T. Takahashi, H. Suganuma, Phys. Rev. Lett. **90**, 182001 (2003)

11. R.K. Bhaduri, L.E. Cohler, Y. Nogami, Nuovo Cimento A **65**, 376 (1981)
12. L. Ya. Glozman, W. Plessas, K. Varga, R.F. Wagenbrunn, Phys. Rev. D **58**, 094030 (1998)
13. F. Brau, C. Semay, B. Silvestre-Brac, Phys. Rev. C **66**, 055202 (2002)
14. B.O. Kerbikov, Yu.A. Simonov, Phys. Rev. D **62**, 093016 (2000)
15. I.M. Narodetskii, M.A. Trusov, Yad. Fiz. **65**, 949 (2002); Phys. Atom. Nucl. **65**, 917 (2002)
16. M. Fabre de la Ripelle, M. Lassaut, Few-Body Systems **23**, 75 (1997)
17. M. Abramowitz, I.A. Stegun, Handbook of mathematical functions (Dover publications, New York 1970)
18. P. Nunberg, D. Prosperi, E. Pace, Nucl. Phys. A **285**, 58 (1977)
19. B. Silvestre-Brac, R. Bonnaz, C. Semay, F. Brau, Quantum three-body problems using harmonic oscillator bases with different sizes, ISN Grenoble, ISN-00-66, 2000 (unpublished)